Short communication

Development of Zn-SiC composite coatings: Electrochemical corrosion studies

Mudigere Krishnegowda Punith Kumar, Thimmappa Venkatarangaiah Venkatesha[✉] and Mudigere Krishnegowda Pavithra

Department of Chemistry, Kuvempu University, Shankaraghatta-577451, Shimoga, Karnataka, India

[✉]Corresponding Author: E-mail: drtvvenkatesha@yahoo.co.uk; Tel.: +91-9448855079

Abstract

The Zn-SiC composite coatings were fabricated by using sulphate plating bath dispersed with 1, 2 and 3 g L^{-1} of 64.28 nm SiC nanoparticles. Appreciable influence on morphology and microstructure was observed in scanning electron microscopy, X-ray diffraction spectroscopy and texture co-efficient calculations for SiC incorporated zinc coatings. The electrochemical corrosion behavior of zinc and Zn-SiC composite coatings was studied by potentiodynamic polarization and electrochemical impedance analysis. Significant reduction in corrosion current and corrosion rate with increased charge transfer resistance was noticed for composite coatings. The SiC incorporated zinc coatings shown improved micro-hardness property to pure zinc coating. The properties of Zn-SiC composite coatings were compared with that of pure zinc coating.

Keywords
SiC nanoparticles; Electrodeposition; Zn-SiC composite coatings; Corrosion

---

Introduction

Zinc has been utilized as a sacrificial layer to protect steel from corrosion. However, the life span of zinc coating is limited in aggressive environment. Consequently, considerable efforts have been made to advance their corrosion resistance property along with other mechanical and physical properties. One of the possible solutions for this is the incorporation of inert particles (nano or micro sized) into a growing Zn metal matrix during electrodeposition. The second phase particles incorporated metal coatings are called as metal matrix composites (MMCs) and these coatings are renowned for their unique functional properties such as corrosion resistance and wear, hardness, magnetic and semiconducting properties compare to pure metal coating [1,2].

Also co-deposition of second phase or inert particles with growing metal matrix is environmentally friendly compared to surface modifications using organic chelating agents and hazardous post plating treatment like chrome passivation [3]. The fabrication of MMCs can be achieved by various methods such as electrodeposition, electroless plating, hot dipping, chemical and physical vapor deposition, stir casting and plasma spraying techniques. Among these techniques, electrodeposition has advantages like low cost, room-temperature operation, single step, good reproducibility and ecofriendly. The nanoparticles like TiO_2 [4], ZrO_2 [5], CeO_2 [6] and SiO_2 [1] were used to prepare Zn metal matrix composites and their mechanical and electrochemical behavior have been studied.

However, the silicon carbide (SiC) nanoparticles are well known for their high chemical stability, high temperature resistance and strong heat impact resistance [7]. In literature, substantial reports are accessible on use of SiC nanoparticles along with nickel matrix to improve mechanical and electrochemical properties of nickel deposits [8-10]. However, not many reports are available on the generation of Zn-SiC composite coatings. Swiderska-Sroda *et al.* [11] used SiC nanoparticles to generate Zn-SiC composite coatings and analyzed their surface appearance and Gabriella Roventi *et al*. [12] studied the effect of SiC incorporation on the morphology and micro hardness of zinc matrix of Zn-SiC composite coatings developed by acidic chloride bath. Nevertheless, the influence of SiC particles on the corrosion behavior of zinc deposit has not been explored. Hence, the present work has been accomplished to investigate the effect of SiC particles on the corrosion behavior of zinc deposit. The Zn-SiC composite coatings were generated by means of electrodeposition method and also their morphological and electrochemical behavior were studied.

Experimental

Deposition process

Zn and Zn-SiC composite coatings were generated on mild steel specimen from zinc plating bath given in the Table 1, which contains separately 0, 1, 2 and 3 g L^{-1} of suspended SiC (64.28 nm) nanoparticles. The plating solutions were mechanically agitated for 24 h by a magnetic stirrer to attain uniform dispersion of SiC nanoparticles in plating bath. The electrodeposition process was carried out at current density of 0.04 A cm^{-2} [2] for 10 min with a solution stirring speed of 300 rpm.

Table 1. *Optimized plating bath composition and operating parameters used for zinc and Zn-SiC composite coating process*

Bath	Constituents	Concentration, gL^{-1}	Deposit code	Operating parameters
Basic bath (BB)	$ZnSO_4$	200	Z	Anode: Zinc plate Cathode: Mild steel plate Current density: 0.04 A cm^{-2} Plating time: 10 min pH 3.5 Temperature: 27 ± 2 °C
	Na_2SO_4	10		
	H_3BO_3	8		
	CTAB	0.05		
B_1	SiC nanoparticles +BB	1.0	ZS_1	
B_2	SiC nanoparticles +BB	2.0	ZS_2	
B_3	SiC nanoparticles +BB	3.0	ZS_3	

Surface characterization

The surface morphology of the coating was investigated using JOEL JEM 1200 EX II Scanning electron microscopy (SEM) and the TiO_2 particle content in the coated film was determined by Energy dispersive X-ray (EDX) analysis coupled with SEM. X-ray diffraction (XRD) analysis of electrodeposits was carried out using Philips TW3710 X-ray diffractometer with Cu Kα radiation (λ = 0.1540 nm) working at 30 mA and 40 kV.

Electrochemical corrosion studies

The electrochemical corrosion studies were performed in a conventional three electrode glass cell by using CHI 660C electrochemical work station (US make) at 27±2 °C. A saturated Ag/AgCl electrode and a platinum wire served as the reference and counter electrode respectively. The coated specimens were used as working electrode with 1 cm^2 exposure area and were immersed in the corrosive media for about 30 min before polarization and impedance measurements to ascertain the steady state potential or open circuit potential (OCP). For the corrosion studies, 3.5 % NaCl solution was used as corrosive media.

Tafel curves for coatings were obtained by applying potential between -200 and +200 mV from their OCP value. Electrochemical Impedance Spectroscopic (EIS) behavior of coatings was measured at their OCP, and the sinusoidal signal amplitude of 5 mV was employed with an alternating current of frequency range from 100 kHz to 10 mHz at 6 points per decade. The measured EIS data were curve fitted and analyzed with the help of commercial ZSimpWin 3.21 software to obtain impedance parameter. Each experiment was repeated thrice to confirm the reproducibility.

Micro-hardness measurements

The micro-hardness of the Zn and Zn-TiO$_2$ composite coatings were measured by Vickers indenter using the instrument "Clemex micro-hardness tester", by forcing a diamond indenter having the geometry as Vickers pyramid, applying the test load 100 g on the individual specimen. The indentation time was 30 s on each specimen surface for the individual load.

Results and discussion

Characterization and surface analysis

The zinc plating bath solutions (Table 1), each containing 0, 1, 2, and 3 g L^{-1} of SiC respectively, were prepared and stirred for 24 h for the uniform dispersion of nanoparticles. The Zn-SiC composite coatings were obtained on mild steel using operating conditions given in Table 1 and the deposits were named in different deposit code and are given in same table. The thickness of the Zn and Zn-SiC MMCs was calculated by using the Equation 1. The corresponding thickness of the deposits is 14.72, 15.24, 15.51 and 15.58 μm for Z, ZS$_1$, ZS$_2$ and ZS$_3$ coatings, respectively.

$$T = \frac{m}{Ad} \tag{1}$$

where *m* is the mass of the deposit, *A* is the area (cm^2) and *d* is the density of the coated metal.

The presence of SiC nanoparticles in the zinc matrix was tested by analyzing the EDX spectra recorded on the Zn-SiC metal matrix composite coatings. The peak corresponds to Si and C in the EDX spectra (Figure 1) recorded at different points on composite coating surface confirms the presence of SiC nanoparticles in zinc matrix. The weight percent of silicon carbide nanoparticles in Zn-SiC MMCs was calculated from the given equation (Equation 2) [12] using the percentage of Zn and Si values obtained from EDX analysis.

$$w_{SiC} = \frac{w_{Si} + \dfrac{w_{Si}}{PA_{Si}} PA_C}{w_{Zn} + w_{Si} + \dfrac{w_{Si}}{PA_{Si}} PA_C} \tag{2}$$

where PA_{Si} and PA_C are Si and C atomic weights respectively and w_{Si} and w_{Zn} are mass fractions obtained from EDX data.
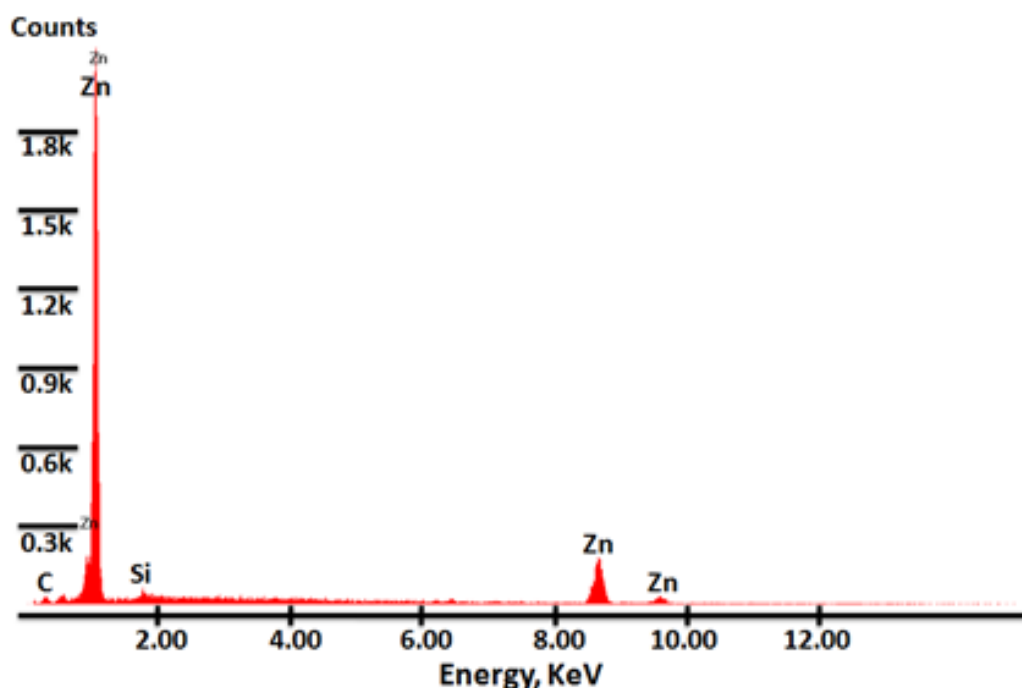
Figure 1. *EDX spectra of Zn-SiC composite coating ZS$_2$*

Weight percent of SiC nanoparticles in the deposit is given in Table 2. It can be observed from Table 2 that the amount of SiC nanoparticles in zinc matrix is slightly increased with an increase in the concentration of SiC nanoparticles in the plating bath. About 0.4799 wt% of SiC particles are embedded in the zinc matrix obtained from the bath solution containing of 2 g L^{-1} nano particles. Figure 2 represents the SEM micrographs of zinc and Zn-SiC MMCs. The randomly distributed, hexagonal zinc platelets without having any local defects were observed in zinc and Zn-SiC deposits but comparatively improved compactness and uniformity was noticed in composite coatings.

Table 2. *Weight percent of SiC present in the composite coatings obtained from EDX analysis.*

coating	ZS$_1$	ZS$_2$	ZS$_3$
	Amount, wt%		
C K*	1.93	1.98	2.01
Si K*	0.30	0.33	0.32
Zn K*	97.77	97.69	97.67
Total	100.00	100.00	100.00
SiC	0.4361	0.4799	0.4655

*K shows the peaks generated by X-rays given off as electrons return to the K electron shell

XRD patterns were obtained for pure zinc and Zn–SiC MMCs to know the influence of SiC nanoparticles on the average crystallite size and orientation of zinc crystals, and are provided in Figure 3. The peaks in diffraction pattern correspond to the zinc hexagonal crystal structure (JCPDS card number 04-0831). The peak correspond to SiC nanoparticles were not observed in diffraction patterns, this may be due to the little incorporation (≈0.45 %, from EDX analysis) of SiC nanoparticles in to Zn matrix. The average grain size of the deposited films was calculated using the Scherrer equation by considering the (101) plane peak broadening (Equation 3) [13].

$$L = \frac{K\lambda}{\beta \cos\theta} \qquad\qquad (3)$$

where *L* - average crystal size, *K* - Scherer constant, λ - wavelength of scattering, β - full width half maxima and θ - scattering angle.
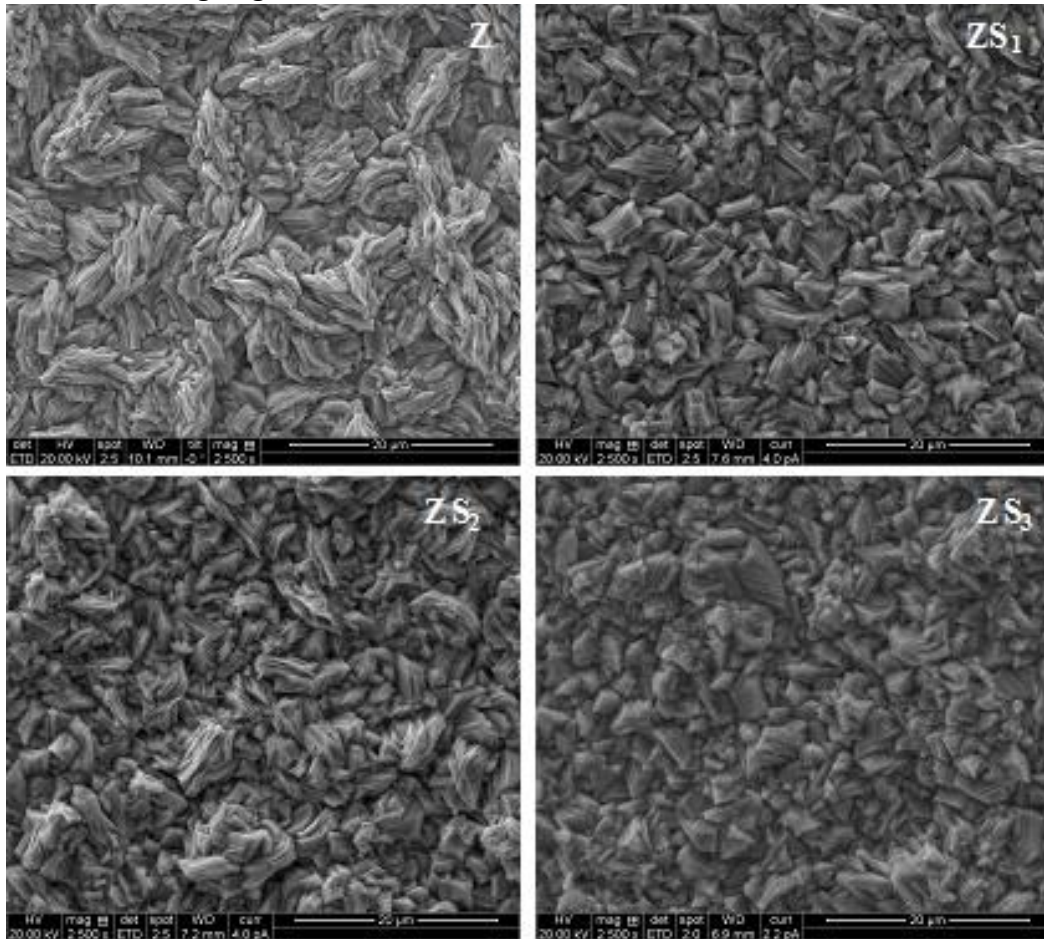

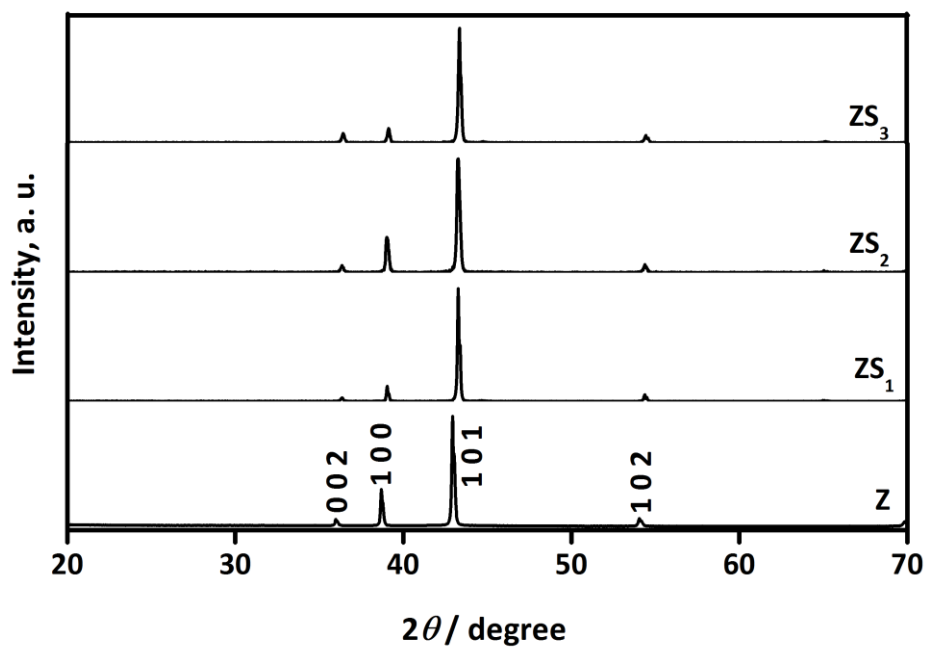**Figure 2.** *SEM micrographs of as deposited zinc and Zn-SiC composite coatings*

Figure 3. *XRD diffractograms obtained from zinc and Zn-SiC composite coatings*

The calculated average crystallite size using Scherrer equation is 89.95, 94.69, 48.80 and 114.76 nm for Z, ZS_1, ZS_2 and ZS_3 deposits, respectively. It can be seen that the inclusion of silicon carbide nanoparticles, significantly influence the grain size of deposit. The change in grain size of the MMCs can be related to the modification of the competition between nucleation and crystals growth in the presence of nanoparticles [4]. The incorporated SiC nanoparticles impede the crystal growth by inhibiting the diffusion of adatoms towards the growing centers and which leads to fresh nucleation [4]. However, in the present work, decrease in average crystal size was observed for ZS_2 coating, i.e., for zinc coating, the average crystallite size is 89.95 nm but it is reduced to 48.80 nm for ZS_2. However in ZS_1 and ZS_3 coatings, the grain size is not reduced by the SiC nanoparticles but they impart compactness to the MMCs.

According to literature, the incorporation of second phase particles to growing metal matrix will alter the preferred orientation of the deposit [4,14]. Texture co-efficient values are calculated by using Equation 4 [15] for all the XRD profiles and the obtained texture co-efficient values are plotted in Figure 4.

$$T_c(hkl) / \% = \frac{I(hkl)}{\sum I(hkl)} \times \frac{\sum I_o(hkl)}{I_o(hkl)} \times 100 \qquad (4)$$

where, T_c(hkl) is the texture coefficient; I(hkl) is the peak intensity of the zinc electrodeposits; $\sum I$(hkl) is the sum of intensities of the independent peaks and the index 'o' refers to the intensities for the standard zinc sample.
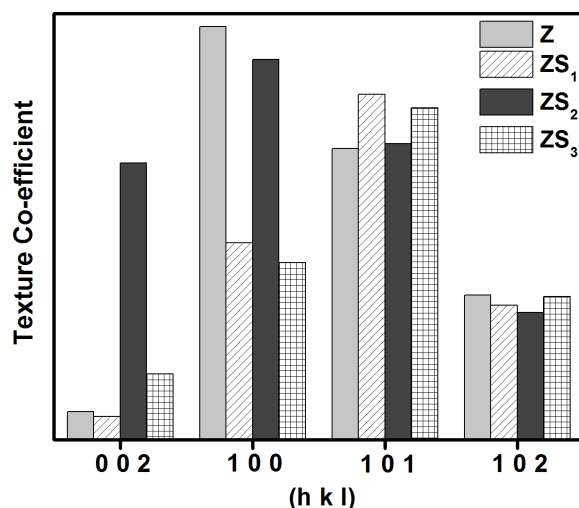

Figure 4. Preferred orientation of crystallites in zinc and Zn-SiC composite coatings.

The preferred orientation plot in Figure 4 reveals that in the zinc deposit, orientation of the zinc crystals is dominated in the (100) plane, however it is changed to (101) plane after the incorporation of SiC nanoparticles into the zinc matrix.

The change in compactness, average crystallite size and texture co-efficient corresponds to Zn-SiC MMCs with respect to pure zinc coating reveals the significant influence of SiC nanoparticles on the morphology and microstructure of the deposits.

Electrochemical corrosion analysis

Characterization studies confirm that the incorporation of SiC particles to zinc matrix influence the morphology and microstructure of the deposits. And the electrochemical corrosion analysis

was carried out in order to compare the effect of morphological and microstructural changes on the quality of Zn-SiC MMCs with respect to the zinc coating.

Potentiodynamic polarization analysis

Polarization measurements were carried in order to examine the influence of SiC nanoparticles on the corrosion behavior of the zinc deposits. The potentiodynamic polarization measurement was performed after 30 min immersion in 3.5 % NaCl corrosive media. The potentiodynamic polarization curves or Tafel plots were recorded for all the deposits in a potential range of ±200 mV from OCP of the corresponding deposit and are given in Figure 5. The extrapolation on these curves resulted in the determination of corrosion parameters such as corrosion poten-tial (E_{corr}), corrosion current (I_{corr}), corrosion rate (CR), and anodic and cathodic slopes (β_a and β_c) and are tabulated in Table 3.

The decreased corrosion current and little drift in corrosion potential towards positive side for ZS_1, ZS_2 and ZS_3 reveal that the Zn-SiC composite coatings are more resistive towards corrosive media than pure zinc coating. In particular, 80 % decrease in corrosion rate is noticed for ZS_2 deposit. The change in anodic and cathodic Tafel co-efficient values of Zn-SiC composite coatings compare to pure zinc coating indicates that the presence of SiC nanoparticles in the zinc matrix influence the kinetics of both anodic and cathodic electrochemical reactions.
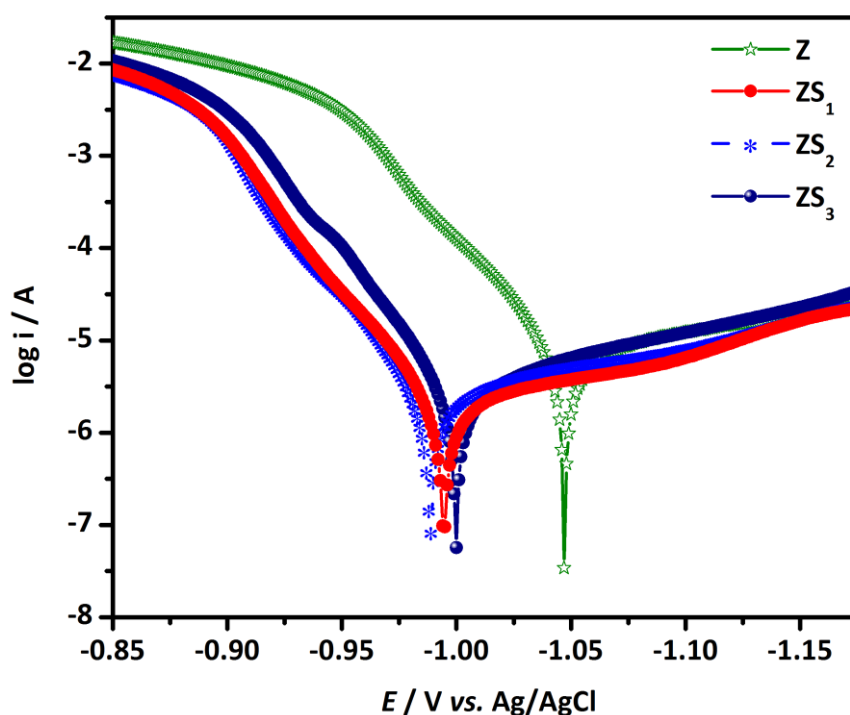

Figure 5. *Potentiodynamic polarization curves for zinc and Zn-SiC composite coatings measured with respect to sat. Ag/AgCl electrode in 3.5 % NaCl solution.*

Table 3. *Electrochemical kinetic parameters of the zinc and Zn-SiC composite coatings derived from Tafel plots.*

Specimen	E_{corr} / V	I_{corr} / μA cm^{-2}	β_c / mV dec^{-1}	β_a / mV dec^{-1}	Corrosion rate, μg h^{-1} cm^{-2}
Z	-1.047	8.505	280	35.72	10.06
ZS_1	-0.995	2.802	248	32.80	3.314
ZS_2	-0.989	2.215	182	32.92	2.620
ZS_3	-1.000	3.526	192	36.69	4.170

Electrochemical impedance analysis

The impedance measurement is the nondestructive and most informative method to assess the corrosion behavior of metal coating. In the present work, the impedance measurement was carried out for all coatings at their open circuit potential in the 100 kHz to 10 mHz frequency range. Initially working electrode was left for 30 min to attain equilibrium potential in 3.5 % NaCl solution before EIS measurement.

The measured electrochemical impedance (EIS) data are presented as Nyquist and typical Bode plots in Figure 6(a) and Figure 6(b) respectively. Two capacitive loops or two time constants corresponds to corrosion process are observed in the Nyquist and Bode plots. The shape of the spectra is influenced by the electrochemical process at the surface and/or by the geometric factors of the electrode [16]. Hence to obtain electrochemical parameters, the experimentally determined EIS data were fitted with a suitable electrical equivalent circuit (EEC) given in Figure 7, with the help of the ZSimpWin 3.21 software. To get appreciable fitting results the employed high frequency capacitance element (C) in EEC was replaced by constant phase element (CPE). The impedance of CPE is defined as

$$Z(i\omega) = (Q)^{-1} (i\omega)^{-n}$$

where Q is the CPE constant, i is the imaginary unit, ω is the angular frequency ($\omega=2\pi f$, f is the frequency) and 'n' is the CPE exponent (where 'Q' and 'n' are frequency independent parameters). The value of 'n' lies between −1 and 1 (*i.e.*, −1≤ n ≤1), for ideal capacitor $n = 1$, for ideal inductor $n =−1$, if $n = 0$ the CPE is ideal resistor [17, 18].
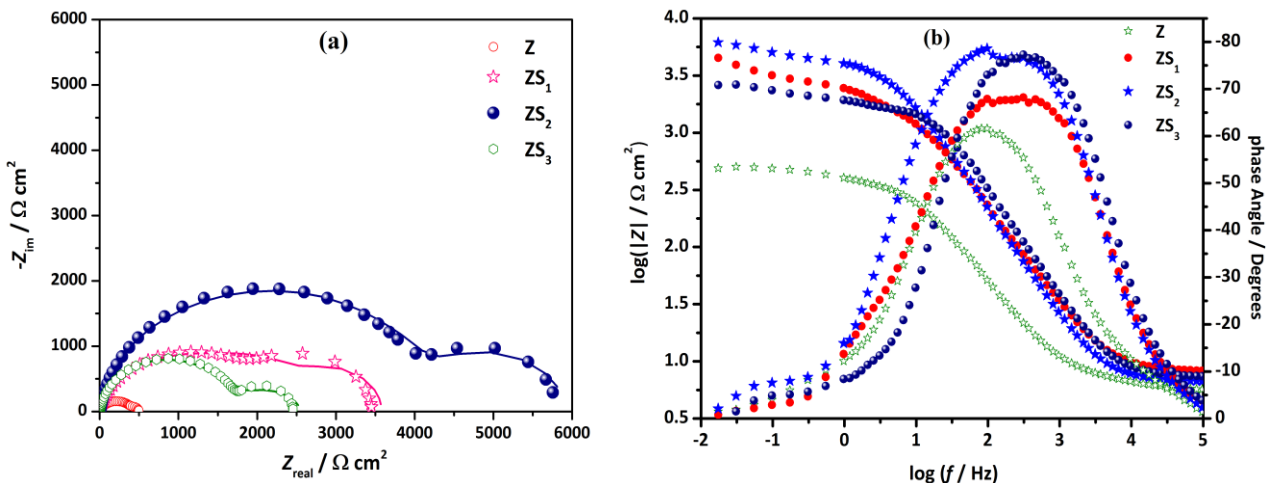

Figure 6. *Impedance (a) Nyquist and (b) Bode plots for zinc and Zn-SiC composite coatings measured with respect to Sat. Ag/AgCl electrode in 3.5% NaCl solution.*
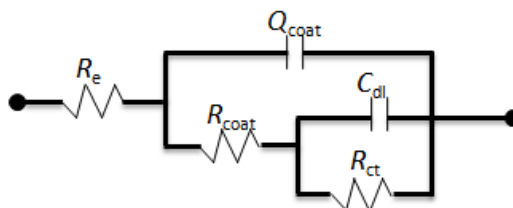

Figure 7. *Electrical Equivalent Circuit used to simulate the recorded Impedance Nyquist plots.*

The contribution of each element in the used EEC is as follows [19].

R_e is the electrolyte resistance that appeared between the reference electrode and the surface working electrode. The high frequency contribution (Q_{coat}–R_{coat}) is ascribed to the dielectric

character Q_{coat} of the coating that is reinforced by ionic conduction through its pores R_{coat}. The low frequency contribution is attributed to the double layer capacitance (C_{dl}) at the electrolyte/coated surface interface at the bottom of the pores coupled with the charge transfer resistance (R_{ct}).

The obtained corrosion parameters are tabulated in Table 4. The polarization resistance was calculated by adding R_{coat} and R_{ct} of the corresponding deposits. The constant phase element is considered as capacitor because the value of CPE exponent '$n \approx 1$'. The extent of anticorrosive nature of the deposit can be analyzed by the resistance offered by the deposit, considering both coating resistance and charge transfer resistance. The polarization resistance exhibited by the pure zinc coating Z is 494.8 Ω cm^2. The incorporation of SiC particles significantly influenced on the polarization resistance of Zn-MMCs coatings *i e*., 3570, 5795 and 2449 Ω cm^2 for ZS$_1$, ZS$_2$ and ZS$_3$ coatings respectively. It should be noted that, SiC incorporated zinc coatings exhibited more resistance for charge transfer with minimum double layer capacitance value when compared to pure zinc coating. The decrease in double layer capacitance value suggests that the electroactive behavior of the surface in corrosive environment is minimum and hence MMCs are much resistive towards external aggressive media. Among all, ZS$_2$ deposit showed tenfold increase in R_{ct} value with decrease in C_{dl} value to the same extent.

The two capacitive loops which were observed in the Nyquist plot are also observed in Bode plots. The impedance modulus $|Z|$ *vs.* the frequency plot shows that impedance modulus value of the composite coatings are greater than that of Z coating, and it is in accordance with the trend observed in polarization and Nyquist plot analysis.
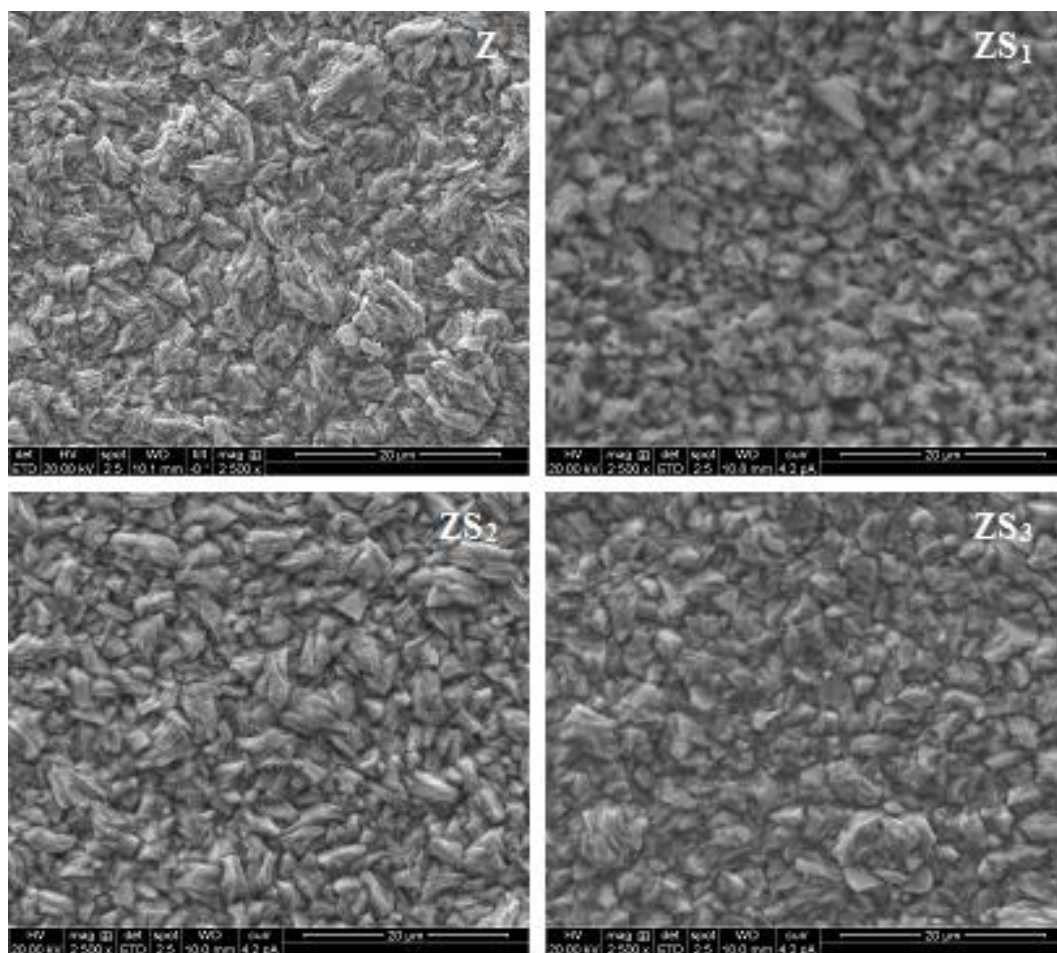

Figure 8. *SEM micrographs of zinc and Zn-SiC composite coatings recorded after potentiodynamic polarization measurement.*

4. *Electrochemical corrosion parameters obtained from EEC simulation of impedance Nyquist plots.*

Specimen	C_{coat} / $\mu\Omega^{-1}$ cm^{-2} S^{-n}	n_{coat}	R_{coat} / Ωcm^2	R_{ct} / Ω cm^2	C_{dl} / 10^{-3} F cm^{-2}	*R_p / Ω cm^2
Z	29.14	0.817	419.6	75.2	6.968	494.8
ZS$_1$	16.38	0.864	2530	1040	0.340	3570
ZS$_2$	13.31	0.931	4188	1607	0.451	5795
ZS$_3$	6.784	0.946	1768	681	0.692	2449

*$R_p = R_{coat} + R_{ct}$

Also the SEM images of the deposits after polarization (Figure 8) shows that the composite coating surface is less deteriorated and retained its compactness when compare to pure zinc coating. Furthermore, the uniform corrosion process was observed on all deposit surfaces and it confirms the defect free nature of the zinc coatings. If deposit has defects then the pitting corrosion behavior is expected.

It is already reported that, the inclusion of SiC nanoparticles to zinc matrix will improve the mechanical properties of the deposit [12]. However, the results gathered from the present work confirm that the incorporation of SiC nanoparticles also enhance the corrosion resistance property of the zinc coatings.

The dissolution of metallic coating depends on the texture, morphology and chemical composition of the deposit [14,20]. Under aggressive environment, the dissolution activities vary because of the difference in binding energy of atoms between the crystallographic planes. The deposits having the crystallographic planes with higher number of adjacent atoms requires higher energy to breakdown the atoms followed by their dissolution. Therefore more energy is required to breakdown the close packed planes or low-index planes because they are associated with high bonding energy of the surface atoms [20].

All the coatings in particular ZS$_2$ exhibit maximum orientation in (100) and (101) planes. So all the coatings including pure zinc coating has to show high corrosion resistance. But better anticorrosion behavior was noticed for composite coatings in particular ZS$_2$, Because Since the different texture and grain boundary distribution of the coating also influences on the corrosion behavior of the coatings. As a result, we observed different corrosion resistance property for zinc coatings.

Micro-Hardness analysis

The measured Vickers micro-hardness value for Zn and Zn-SiC MMCs is given in Figure 9. The given micro-hardness values were an average of 5 measurements performed on different locations at the centre portion of coated samples.

The slightly increased micro-hardness value was observed for Zn-SiC MMCs compared to pure zinc coating, because of the minimum incorporation of SiC nanoparticles in metal matrix. Also, it can be observed that there is no significant difference in micro-hardness value between ZS$_1$, ZS$_2$ and ZS$_3$ coating. It may be due to the percentage of SiC incorporation is comparatively equal in all the MMCs. However, MMCs exhibit better micro-hardness value compared to that of pure zinc coating. It can be supposed that nanoparticles co-deposited in the composite coating might act as barriers to impede the plastic deformation of Zn matrix and hence enhance the micro hardness [21].
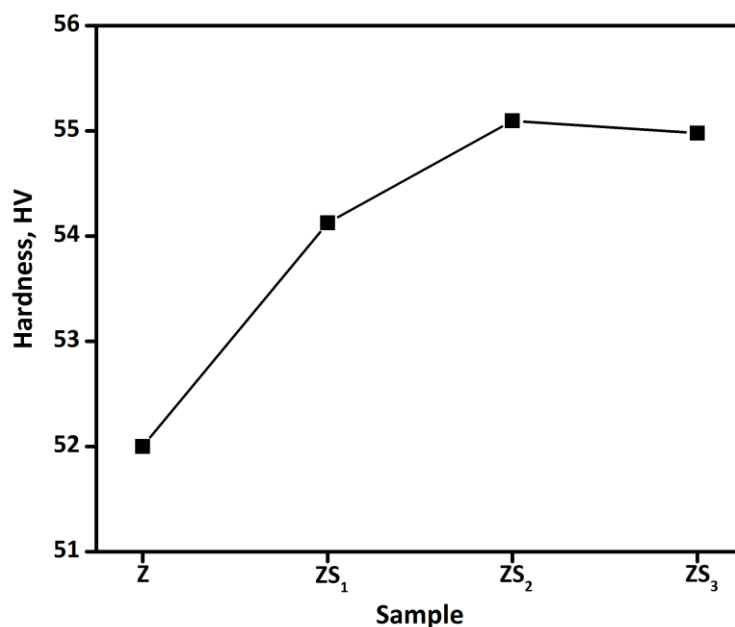
Figure 9. *Vickers micro-hardness value of Zn and Zn-SiC MMCs.*

Conclusions

The Zn-SiC composite coatings were successfully generated on mild steel by electrodeposition method. The SEM and XRD analysis demonstrate that, the incorporation of SiC nanoparticles considerably change the morphology and microstructure of the deposits. The preferred orientation of the zinc crystallites in SiC incorporated coatings is changed to (101) plane from (100) plane of the zinc crystallite in pure zinc coating. Also uniform and compact nature was observed in Zn-SiC MMCs. The incorporation of SiC nanoparticles in to zinc metal matrix improved the micro-hardness property of the deposit. The electrochemical corrosion studies reveal that Zn-SiC composite coatings have better corrosion resistance property than pure zinc coating. Compare to pure zinc coating, 60 to 80% decrease in corrosion rate was observed for composite coatings; in particular, ZS_2 coating has significant resistance towards external aggressive media. The passive barrier behavior of uniformly distributed SiC nanoparticles and morphological changes may responsible for the anticorrosive behavior of the Zn-SiC MMCs.

References

[1] T- J. Tuaweri, G. D. Wilcox, *Surf. Coat. Technol.* **200** (2006) 5921-5930.
[2] C. M. Praveen kumar, T. V. Venkatesha, K. G. Chandrappa, *Surf. Coat. Technol.* **206** (2012) 2249-2257.
[3] C. B. Wang, D. L. Wang, W. X. Chen, Y. Y. Wang, *Wear.* **253** (2002) 563-571.
[4] A. Vlasa, S. Varavara, A. Pop, C. Bulea, L. M. Muresan, *J. Appl. Electrochem.* **40** (2010) 1519–1527.
[5] K. Vathsala, T. Venkatarangaiah Venkatesha, *Appl. Surf. Sci.* **257** (2011) 8929-8936.
[6] S. M. A. Shibli, F. Chacko, *Surf. Coat. Technol.* **202** (2008) 4971-4975.
[7] H. Chang, T. T. Tsung, L. C. Chen, C. S. Jwo, J. W. Tsung, Y. C. Lu, *J. Mater. Eng.* Perform, **14** (2005) 158-162.

[8]   F. Hu, K. C. Chan, S. Z. Song, X. J. Yang, *J. Solid State Electrochem.* **11** (2007) 745–750

[9]   M. R. Vaezi, S. K. Sadrnezhaad, L. Nikzad, *Colloid. Surface A: Physicochem. Eng. Aspects.* **315** (2008) 176-182.

[10] S. K. Kim, H. J. Yoo, *Surf. Coat. Technol.* **108**-**109** (1998) 564-569.

[11] A. Swiderska-Sroda, J. A. Kozubowski, A. Maranda-Niedbala, E. Grzanka, B. F. Palosz, A. Presz, S. Gierlotka, S. Stelmakh, G. Kalisz, N. Herlin-Boime, C. Lathe, *Solid State Phenomena.* **101-102** (2005) 151-156.

[12] G. Roventi, T. Bellezze, R. Fratesi, *J. Appl. Electrochem.* **43** (2013) 839– 846.

[13] A. L. Patterson, *Phys. Rev.* **56** (1939) 978–82.

[14] K. O. Nayana, T. V. Venkatesha, B. M. Praveen, K. Vathsala, *J. Appl. Electrochem.* **41** (2011) 39–49.

[15] M. Mouanga, L. Ricq, J. Douglade, P.Berçot, *Corros. Sci.* **51** (2009) 690–698.

[16] F. La Mantia, J. Vetter, P. Nov´ak, *Electrochim. Acta.* **53** (2008) 4109–4121.

[17] J. Macak, P. Sajdl, P. Kucera, R. Novotny, J. Vosta, *Electrochim. Acta.* **51** (2006) 3566–77.

[18] A. K. Mishra, R. Balasubramaniam, S. Tiwari, *Anti-Corros. Method. M.* **54(1) (**2007) 37–46.

[19] S. Ranganatha, T. V. Venkatesha, *RSC Adv.* **4** (2014) 31230–31238.

[20] H. Park, J. A. Szpunar, *Corr. Sci.* **40** (1998) 525-545.

[21] L. M. Chang, M. Z. An, H. F. Guo and S. Y. Shi, *Appl. Surf. Sci.* **253** (2006) 2132-2137.